Turbulence and Signal Analysis

Pierre Borgnat (email Pierre.Borgnat@ens-lyon.fr)
Laboratoire de Physique (UMR-CNRS 5672) ÉNS Lyon 46 allée d'Italie 69364 Lyon Cedex 07

Abstract

Turbulence deals with the complex motions in fluid at high velocity and/or involving a large range of length-scales. Turbulence asks then many questions from modeling this complexity to measuring it. In a first part, the description of signals measured in fluid turbulence experiments will be made along with a survey of modern signal processing tools that are adapted to their properties of scaling laws, multifractalty and non-stationarity. A second part will be devoted to the study of one signal processing framework, the decomposition of self-similar signals on the Mellin oscillating functions, that is a new way to probe jointly scale invariance and local organization of a signal.

1 Turbulence: experimental signals and signal processing tools

1.1 Preliminary analysis of fluid turbulence

Formalization of the problem. Turbulence is first a problem of fluid mechanics [Bat67]. Let $\mathbf{u}(\mathbf{r}(0);t)$ be the Lagrangian velocity of a fluid element that is in $\mathbf{r}(0)$ at initial time; ρ is its density. It obeys the fundamental relation of dynamics: $\rho D_t \mathbf{u} = \sum \rho \mathbf{f}$, where $\mathbf{f}$ are the forces: friction, pressure forces, gravity ($\mathbf{f} = \rho \mathbf{g}$),... This equation is linear but non-local because of the pressure term. If p is the pressure, the corresponding force is $-\nabla p$ which is linked to the whole velocity field. Added to that, it is experimentally hard to track the movement of one fluid element in a fluid. So, instead of the Lagrangian velocity, the problem is often studied with the corresponding Eulerian velocity $\mathbf{v}(\mathbf{r},t)$ at the fixed position $\mathbf{r}$. Both velocities are related via the change of variable $\mathbf{u}(\mathbf{r}(0);t) = \mathbf{v}(\mathbf{r}(t);t)$. The equation for the Eulerian velocity, called the Navier-Stokes (NS) equation, reads then as:

$$D_t \mathbf{v} = \underbrace{\partial_t \mathbf{v}}_{\text{local derivative}} + \underbrace{(\mathbf{v}\cdot\nabla)\mathbf{v}}_{\text{convective derivative}} = -\frac{1}{\rho}\nabla p + \underbrace{\nu \Delta \mathbf{v}}_{\text{viscuous friction}} + \sum \mathbf{f}_v. \tag{1}$$

Friction in the fluid (supposed newtonian) is explicitely written here and it is proportional to the vicosity ν. For an uncompressible flow, the continuity equation $\nabla\cdot\mathbf{v} = 0$ completes the problem. Remark that the pressure term is non-local because of a Poisson equation that relates p to $\mathbf{v}$: $\Delta p = -\partial^2(v_i v_j)/\partial x_i \partial x_j$. One should also specify the boundary conditions: the velocity of the fluid is zero at the boundaries. One simple approach adopted by physicists is to study turbulence in open systems far from the boundaries in order to find a possible generic behaviour of a turbulent fluid, disregarding the specific geometry of the boundaries.

Signals of Eulerian velocity. Experiments of turbulence consists in studying high speed motions in a fluid where the flow is disturbed by means of a grid or by creating a jet. The flow becomes turbulent, and the velocity of the fluid is recorded along time at some position. Common apparatus are hot-wire probes that measure one component $v(t)$ of the velocity at one point only (we will discuss only single probe measurements here).

A sample velocity signal $v(t)$ is shown in figure 1, obtained during the experiment GReC [PPB$^+$03] in a jet at high Reynolds number (up to 10^7) in helium at 4.5 K (so that its viscosity is very low). The erratic fluctuations are typical of such signals and one can see numerous points where the signal appears almost singular. The singular fluctuations are clearer for the dissipative signal, that is measured as the time derivative of its energy $v(t)^2/2$; it seems made of numerous peaks of variable amplitudes, separated by periods of almost

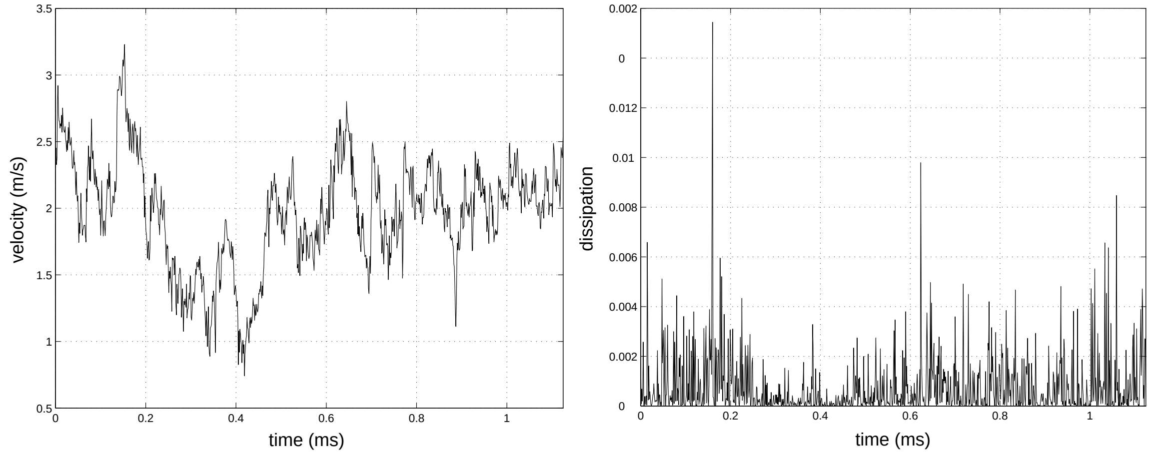

Figure 1: Left: a typical Eulerian velocity signal $v(t)$. Right: its corresponding dissipation (derivative of the squared velocity). Those signals were measured by Pietropinto *et al.* as part of the GReC experiment [PPB$^+$03] of fluid turbulence in low temperature gaseous helium.

no activity: the density of peaks is fluctuating from time to time. This is called spatial intermittency. Lastly, we notice that there exist large-time fluctuations (long excursions far from the mean) as well short-time variations. The question is to undertand all those features.

Dimensional analysis of turbulence. The drawback of the NS equation is that it is non-linear, due to the convective term: one may expect solutions with complicated shapes (as in figure 1). On the other hand, the friction term may impose some regularity on the solutions. The balance between the two effects is obtained by dimensional analysis. Let U be a typical velocity, and L a typical length scale of the full flow (for instance the size of an experiment), then $(\mathbf{v}\cdot\nabla)\mathbf{v} \sim U^2/L$ and $\nu\Delta\mathbf{v} \sim \nu U/L^2$. The ratio is the Reynolds number $\mathrm{Re} = UL/\nu$, and this is the only quantity left if one takes out the dimensions from the variables. When Re is high, the flow becomes irregular and unpredictable, with motions at many difference length scales: the fluid is turbulent. **The symmetries of the equation appear to be broken in the flow: it is disordered spatially and chaotic temporally**.

A key remark is that a turbulent flow is very different from a flow with zero viscocity, even when $\mathrm{Re} \to \infty$ (fully developped turbulence). Indeed, the energy dissipated in the flow is never zero because the irregularity of the solutions increases correspondingly, creating strong gradients in the flow. The dissipation is defined as $\varepsilon = -\mathrm{d}(|\mathbf{v}|^2/2)/\mathrm{d}t$. If the flow is stationary, its mean along the time is constant and equals its spatial mean: $\overline{\varepsilon} =< \varepsilon(\mathbf{r}) >_{\mathbf{r}} = -\nu < |\boldsymbol{\omega}|^2 >_{\mathbf{r}}$; here we introduced the vorticity, $\boldsymbol{\omega} = \nabla \wedge \mathbf{v}$, characterising the swirling motions in the fluid, and $\varepsilon(\mathbf{r}) = \nu(\partial v_j \partial x_i + \partial v_i \partial x_j)^2/2$ is the local dissipation. A first dimensional analysis keeps only $\overline{\varepsilon}$ and ν as relevant parameters. Combining them, Kolmogorov introduced a dissipative length scale $\eta = (\nu^3/\overline{\varepsilon})^{1/4}$ where the solution should become smooth because of the fluid friction. As a consequence, the estimated number of modes (needed for computer simulations) is, for the three-dimensional velocity, $(L/\eta)^3 = \mathrm{Re}^{9/4}$. This number is too high to conveniently use methods from nonlinear dynamical systems. Mathematically speaking, characterising the flow from the NS equation is hard because of all those properties.

An alternative approach in physics is to forget about the dynamical equation and find only the statistical properties of the velocity field [Bat53, BLF53]. Knowing the complete initial velocity field of a turbulent fluid, and then following its proper evolution in time is hopeless because of the high number of modes and of the non-linearity of the equation (it has potential chaotic properties). Experimental observations support this assertion: the fluid seems erratic, with many ever changing currents and eddies, and typical measurements of the Eulerian velocity as a function of time are strongly shambled signals. Forgetting about the initial conditions and exact geometrical setting, one can find simple models to describe statistical properties of the signal, assuming that $\mathbf{v}(\mathbf{r};t)$ is a random process indexed by $\mathbf{r}$ and t. We will review main results obtained by this way, with specific insights about the signal processing tools needed to relate the measurements with the statistical descriptions of a turbulent field.

1.2 Estimation of scaling laws in turbulence

A multiresolution characterisation: the velocity increments. Harmonic analysis of the velocity relies first on its spectral analysis. Fourier representation $v(t) = \int e^{-i2\pi u\nu} \mathrm{d}\xi(\nu)$ is suited especially if v is stationary, in which case its spectrum S_v is given by $\mathbb{E}\left\{\mathrm{d}\xi(\nu_1)\mathrm{d}\xi(\nu_2)\right\} = S_v(\nu)\delta(\nu_1 - \nu_2)\mathrm{d}\nu_1\mathrm{d}\nu_2$ ($\mathbb{E}$ is the expectation). See figure 2 for an estimate of $S_v(\nu)$. The support of the spectrum is broad-band and $S_v(\nu)$ follows roughly a power-law with cut-offs at the inertial scale L, and at the small scale were dissipation becomes dominant (around η). This corresponds to the lack of a single time scale of evolution. The flow has a complex evolution both in time and space. Added to this, the velocity signal is almost Gaussian and does not describe the rare high-intensity events evidenced in dissipation. A Gaussian law of probability and the spectrum are not enough to characterise well the apparent complexity and burstiness of $v(t)$, and so the intermittency.

In order to question all the time scales in the signal, the velocity increment over the time separation (or scale) τ at time t was introduced as a more relevant quantity: $\delta v(\tau; \mathbf{x}, t) = v(\mathbf{x}; t - \tau) - v(\mathbf{x}; t) = v(\mathbf{x} + \mathbf{r}; t) - v(\mathbf{x}; t)$. This quantity is a multiresolution quantity in the sense that it describes the velocity at the varying resolution τ. The second expression for $\delta v(\tau)$ uses the Taylor hypothesis and postulates that the velocity fiels is quickly advected so that there is no (or small) evolution of v during the time τ; this is an hypothesis of “frozen” turbulence during the time scale of the measurement. The increment $\delta v(\tau)$ is then a valid spatial description $\delta v(r)$ with $r = |\mathbf{r}| \simeq \tau|\mathbf{v}(\mathbf{x}; t)| = \tau v$. Velocity increments are relevant to capture both long-time evolution of the signal (dominated by the statistics of v because $v(t - \tau)$ and $v(\tau)$ are then almost independant) and short time behaviour where the dominant features are intermittent peaks of activity evidenced in the derivative of the signal.

Wavelet transform and estimation in turbulence. Velocity increments are not the only multiresolution quantities and in the context of estimation, they are not the most well-behaved. A general class of multiresolution representation is the wavelet transform [Mey90]: $T_v(t, a) = \int v(u)\psi([u - t/a)\mathrm{d}u/a$. Velocity increments are “the poor man’s wavelet”, setting $\psi(u) = \delta(u + 1) - \delta(u)$ and letting τ be the scale variable a. Wavelets are good basis for estimation [AFTV00] because the property of stationary increments is mapped to the stationarity of the coefficients $T_v(t, a)$ and those coefficients decorrelate quickly: the mean of $|T_v(t, a)|^p$ are good estimators for the moments of $\mathbb{E}\,|\delta v(r)|^p$ with $r = a\overline{v}$; moreover the wavelet transforms may be blind to polynomial trend (by using wavelet with more than one zero moment) and are more robust than direct calculus from the velocity increments.

We want to characterise $\delta v(r)$ completely, trying to estimate all its moments. They are called the structure functions: $\mathbb{E}\left\{|\delta v(r)|^p\right\}$. We report in figure 2 some properties of the structure functions: they look like power-laws over the inertial range. At the bottom of this figure, we draw the evolution of the exponents ζ_p of this power-law with the order p of the moment, and the probability density function of the increments $\delta v(r)$ for different r, estimated from the wavelet transform of v.

A further advantage of the wavelet transform is the possibility to use only local maxima of the wavelet coeffficients, that represent best the singularities in the signal (this leads to WTMM for continuous wavelet basis [AM95], or wavelet leaders for discrete basis [Jaf04, Las04]). Indeed, if a signal is singular so that $|v(r) - v(r_0)| \sim |r - r_0|^h$, its wavelet transform verifies $\mathbb{E}\,|T_v(r_0, a)| \sim a^h$ when $a \to 0^+$. The models will rely heavily on singularities, so wavelets are good tools to probe them.

1.3 Statistical modelling of Eulerian turbulence

Self-similarity: The theory of Kolmogorov 41. A short review of the theoretical descriptions of scaling laws in turbulence is needed to understand the experimental analysis. A large litterature on the subject exits, see for instance [Bat53, MY71, Fri95]. In question is a model of the statistical properties of the random variables $\delta\mathbf{v}(\mathbf{r}; \mathbf{x}, t)$. Kolmogorov proposed in 1941 [Kol41a, Kol41b] a full description of velocity postulating that symmetries of the velocity increments are statistically recovered: time stationarity (independance from t), spatial homogeneity (independance from $\mathbf{x}$; note that this is valid because it models turbulence far from the boundaries) and isotropy. To those he adds the property of self-similarity:

$$\delta v(\lambda \mathbf{r}; \mathbf{x}, t) \sim \lambda^{-h} \delta v(\mathbf{r}; \mathbf{x}, t). \tag{2}$$

This last-property is really interesting: this is a description of the regularity and the intermittency of the solution because, if this relation holds for small separations $|\mathbf{r}|$, one solution is to have $\delta v(r) \sim r^h$ which rules the behaviour of the derivative, and consequently of the dissipation. It defines the kind of peaks one expects to find in the dissipation signal.

With those symmetries, the only parameters left are the mean dissipation $\overline{\varepsilon}$, the viscosity ν, the self-similarity exponent h and the length-scale r one considers. Kolmogorov supposes that every spatial scale behaves the same, with the same mean dissipation so that for any r, $\overline{\varepsilon} \sim [\delta v(r)]^2/[r/\delta v(r)]$. Thus $\delta v(r) \sim \overline{\varepsilon}^{1/3} r^{1/3}$: the velocity has a unique exponent of self-similarity $h = 1/3$. The moment of δv should then obey the following relations :

$$\mathbb{E}\left\{|\delta v(r; \mathbf{x}, t)|^p\right\} = C_p (\overline{\varepsilon} r)^{p/3} \text{ if } \eta \preceq r \preceq L \text{ (inertial zone)} \tag{3}$$

When $p = 2$, the scaling law imposes the spectrum of the velocity by means of the Winer-Khinchin relation. Kolmogorov's well-known prediction is that the spectrum should be: $S_v(k) \sim \nu^{5/4} \overline{\varepsilon}^{1/4} (k\eta)^{-5/3}$ if k is in-between $1/L$ and $1/\eta$ (the inertial zone). This last prediction holds well, as seen on figure 2. But the general prediction of (3) is found failing for other orders. $\mathbb{E}\left\{|\delta v(r; \mathbf{x}, t)|^p\right\}$ as a function of r is only rougly a power-law r^{ζ_p} (but not exactly [BCT+93]), and this approximate law has not the exponents $\zeta_p = p/3$ predicted in (3). The evolution exponents with the order p is not linear.

Characterisation in terms of singularities: Multifractal formalism. The failure of K41 is related to the spatial and temporal intermittency of the dissipation: random bursts of activity exist and the regularity of the signal changes from one point to another, and so does ε from one scale to another. The self-similar property (2) holds only in a statistical way where h is also a random variable that depends on $\mathbf{x}$ and t. If this property holds for $\lambda \to 0^+$, h is called the Hölder exponent of the signal at point $\mathbf{x}$. The set of points sharing the same Hölder exponent is a complex random set that is a fractal set with dimension $D(h)$. This is the multifractal model [FP85, Fri95] that describes the signal in terms of singularities at small scale; it supposes then that all the statistics are ruled by their behaviour. The complementary property of the multifractal formalism relates then the singularity spectrum $D(h)$ with the scaling exponents ζ_p by means of a Legendre transform: $D(h) = \inf_p (hp + 1 - \zeta_p)$. Mathematical aspects of multifractality can be found in [Jaf97]. Experimentally, in order to measure the multifractal spectrum that is the core of this model, one has first to compute a multiresolution quantity, then use a Legendre transform that is a statistical measure of $D(h)$ from the exponents ζ_p. Experiments now agree with $\zeta_p \simeq c_1 p - c_2 p^2/2$, where $c_1 \simeq 0.370$ and $c_2 \simeq 0.025$; this is a development in a power series p^n and terms p^n with $n \leq 3$ are too small to be correctly estimated nowadays. The singularity spectrum is then consistent with the log-normal model, and $D(h) = 1 - (h - c_1)^2/2c_2$. The expected value of h is 0.37 on a set of dimension 1 in the signal, but the local exponent fluctuates.

Because the physical velocity should be a continuous signal at small scales (smaller than η), it has been proposed as a further refinement that the complex time singularities with the form $|t - z_0|^{h(t_0)}$, with $z_0 = t_0 + i\zeta \in \mathbb{C}$ could be part of the time signal $v(t)$, and the basis for multifractal interpretation. Such a distribution of singularities having each a spectrum $\sim k^{-2h-1} e^{-2\zeta U k}$ lead to a mean spectrum consistent with the K41 prediction and the quantitative measurements. Yet such singularities have not yet be derived directly from the NS equation, but only in simpler dynamical systems [FM81, FMW03].

Characterisation as random cascades. To understand the statistical intermittency of the flow, one may model only the statistics of the flow. A feature of equation (3) is notable: if the equation were true, the random variable $\delta v(r)/(\overline{\varepsilon} r)^{1/3}$ should be independant of r [Cas97]. However experimental measurements of the probability density function (pdf) of $\delta v(r)$ shows that its shape changes with r, even in the inertial domain; see figure 2. At large scale (close to L), the pdf is almost a Gaussian; when probing smaller scale, exponential

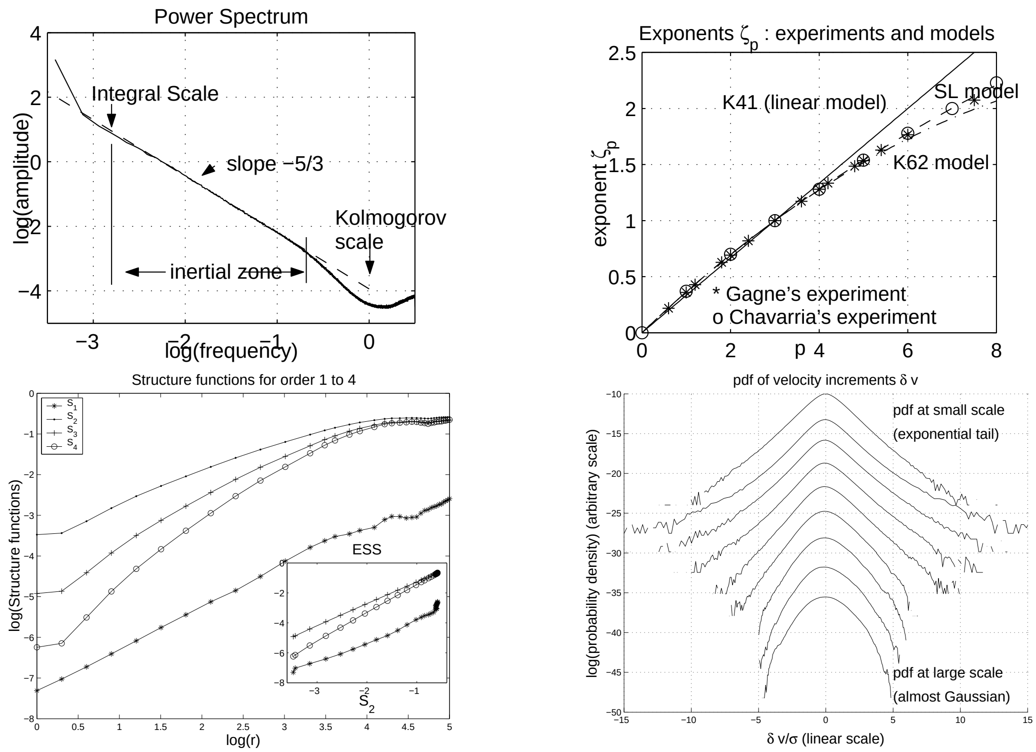

Figure 2: Statistical analysis of one-point velocity measurements. Top left: spectrum $S_v(k)$ of the velocity that follows the K41 prediction of a power-law of exponent 5/3. Bottom left: structure functions $S_p(r) = \mathbb{E}\,|\delta v(r)|^p$ for $p = 1$ to 4; inserted is shown the Extended Self-Similarity property: the structure fonctions are not really power laws of r, but better power laws of one another. Top right : exponents ζ_p of the higher-order statistics (taken from [Gag87] and [CBC95]) are shown different from the K41 model, and closer to a multifractal models (here the Kolmogorov-Obhukov model –K62– and the She-Lévêque model). Bottom right: pdf of the increments figured at various scales, from small scale (a few η) where the pdf is non-Gaussian with heavy tails, to large scale (around L) where the pdf is almost Gaussian; note that the scale is logarithmic for the pdf. The experimental spectrum and pdf are from the datas of the GReC experiment [PPB$^+$03].

tails become more and more prominant: rare intense events are more frequent at small scale – this is another face of intermittency.

This property is best modelled as a multiplicative random process, where each scale is derived from the larger one. The general class of this model comes from the Mandelbrot martingales [KP75] and was also developped from the experimental datas in turbulence [Nov71, Cas97]. The defining property is that the probability function $P_r(\ln|\delta v|)$ at scale r satisfies: $P_{r_2}(\ln|\delta v|) = G^{\star[n(r_2)-n(r_1)]} \star P_{r_1}(\ln|\delta v|)$, where $\star$ is a convolution. This is the property of an infinitely divisible process and G is the kernel of the cascade, that is the operator that warps the fluctuations from one scale r_1 to another r_2: $G_{r_1,r_2} = G^{\star[n(r_2)-n(r_1)]}$. From this, one can derive the structure functions and they read:

$$\mathbb{E}\left\{|\delta v(r;\mathbf{x},t)|^p\right\} \sim e^{H(p)n(r)} \text{ with } H(p) = -\ln\tilde{G}(p), \tag{4}$$

($\tilde{G}$ is the Laplace transform of G). A consequence of the model is that if $n(r)$ is close to $\log r$, the structure function obeys a power-law with exponents $\zeta_p = H(p)$. If not, the property is extended self-similarity because all orders share the same law $e^{n(r)}$ and for instance $\mathbb{E}\left\{|\delta v(r;\mathbf{x},t)|^p\right\} \sim \left(\mathbb{E}\left\{|\delta v(r;\mathbf{x},t)|^3\right\}\right)^{H(p)}$ ($\zeta_3 = 1$ because of the Kármán-Howarth equation [Fri95]). The interest of multiplicative cascades seen as infinitely divisible processes is that this leads to effective construction of stochastic processes satisfying exactly the relations (4), and they can be used as benchmark for the estimation tool based on wavelet [BM03, CRA04].

Lastly, a model that links multifractality and infinitely divisibility was built by adding the fact that beneath the dissipative scale η, the velocity is differentiable: $\delta v(r) = r\partial v/\partial x$. In order to do this small scale regularizaton, one has to define a local dissipative scale, obtained when the local Reynolds number $\mathrm{Re}(r) = r\delta v(r)/\nu$ equals 1, to the strength of the local singularity. In fact we have $\delta v(r) \sim (r/L)^{h(\mathbf{x})}U$ if $r > \eta(\mathbf{x})$ so that $\mathrm{Re}(r) = r\delta v(r)/\nu = (l/L)^{1+h(\mathbf{x})}\mathrm{Re}$. The dissipative scale is fluctuating locally as $\eta(h) = L\mathrm{Re}^{-1/(1+h)}$, whereas K41 uses a fixed dissipative scale $\eta = (\nu^3/\bar{\varepsilon})^{1/4}$ which is now the mean of the $\eta(h)$. Given this behaviour, a unified description of the statistics $\mathbb{E}\{|\delta v(r;\mathbf{x},t)|^p\}$ was derived, valid both in the inertial and dissipative scales [Che04, CRL$^+$03]. Still, this description is phenomelogy; no interpretation is given in terms of fluid mechanics.

1.4 Further analysis of turbulence: non-stationarity, vortices and Lagrangian velocity

Vortex models for turbulence and oscillating singularities. Previous models were built on multi-scale properties of the velocity and on its singularities, and they are good description of the datas. These models lack connexion with the NS equation and with the structured organisation of turbulent flows which are far from purely random flows. Another approach is to characterise a flow from its inner structures. Experiments of turbulence show that there are intense vortices: objects similar to stretched filaments around which the particles are mainly swirling [DCB91]. The singularities in velocity signals could then be understood as features of a few organized objects with a complex inner structuration and a singular behaviour near their core [Mof84, JKVF93]. A mechanism could be spiraling structures, close to what a Kelvin-Helmholtz instability creates [Mof93]. Lundgren studied a specific collection of elongated vortices having a spiraling structure in their orthogonal section, and that are solution of the NS equation given a specified strain [Lun82]. It was shown that such a collection could be responsible for a spectrum in $k^{-5/3}$ and intermittency of the structures functions consistent with modern measurements of ζ_p [SP96]. Turbulence would then be some superposition of complex building objects with geometrical characteristics, such as oscillations or fractality (but in a geometrical, not statistical, way).

• A simple model for corresponding Eulerian velocity signals would be an accumulation of complex singularities, complex in the sense that their exponent is complex (and not their initial time as previously proposed): $(t-t_0)^{h+i\beta}$; see some examples of those functions on figure 5. The exponent β is responsible for oscillations in the signal and multifractal estimation is perturbed by such oscillations [ABJM98].

The Fourier spectrum of a function $e^{-a(t-t_0)}(t-t_0)^{h+i\beta}$ behaves like $e^{4\pi\beta \mathrm{atan}(2\pi\nu/a)}|4\pi^2\nu^2 + a^2|^{-h-1}$; except at low frequencies, so when $\nu \gg a$, the spectrum scales like $|\nu|^{-2h-2}$. This is a power law so they can be used as basis functions to built a synthetic signals with properties of turbulence measurements. A sum of many functions of this kind may have multifractal properties that depends on the distribution of the h and β exponents [Bor02]. One is then interested to find whether or not there are such oscillations in velocity signals.

• The consequences of the existence of spiraling strcutures for Lagrangian velocity would be the existence of swirling motions when a particle is close to a vortex core. Far from vortices, the motion should be almost ballistic, with small acceleration. A further consequence is that the motion is not well approximated by a stationary random process and could be better analysed in a non-stationary framework.

• The vortices and the swirling motions are described by the vorticity $\boldsymbol{\omega}$. We have seen that $\boldsymbol{\omega}$ is related to dissipation and if vortices are relevant features of a flow, vorticity should be strongly organized in those specific structures. We should detect them as isolated objects and a question is about their role in intermittency. Heretoo the non-stationary evolution of those objects is an expected feature.

The general problem is that one can not easily track at the same time the three kinds of interesting properties for turbulence: non-stationarity of the signals; the inner oscillating or geometric structure; and the statistical self-similar properties (exponent h or multifractality) of the spiraling vortices or their consequence for velocity [Bor02].

Alternative representations of signals. Dealing with these three properties, we know how to construct a representation jointly suited to two of them at the same time. The third one is then difficult to assess.

1. Time evolution and self-similarity: statistical methods using wavelets are adapted to multifractals or

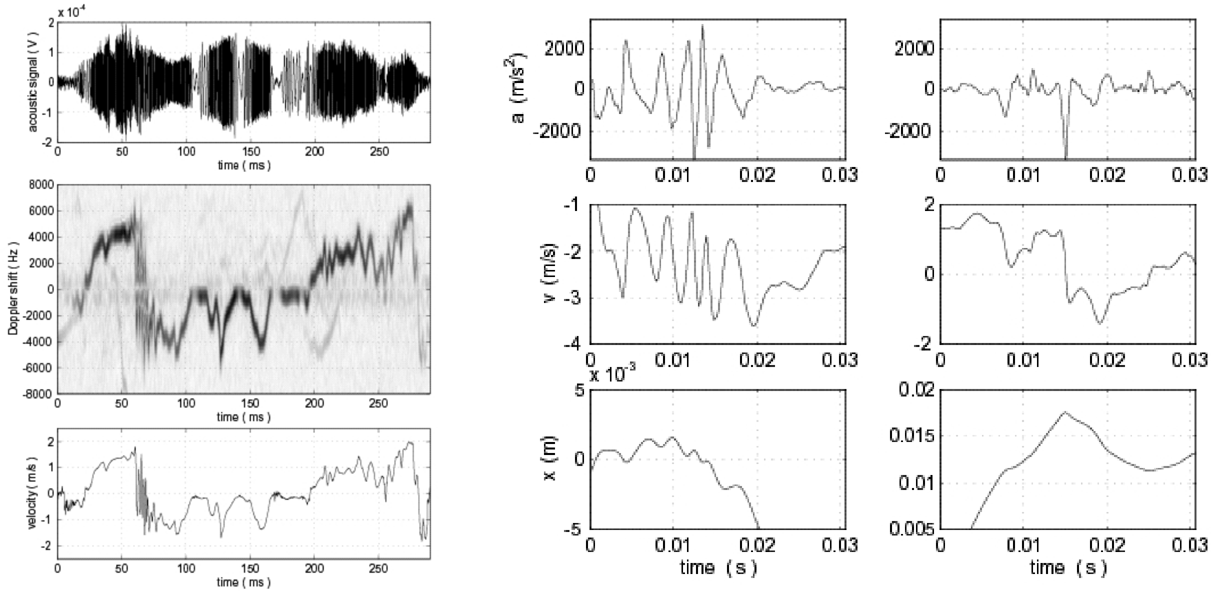

Figure 3: Lagrangian velocity of a particle in turbulence (from [MMMP01]). Left: the Doppler signal whose instantaneous frequency gives the velocity of the tracked solid particle in a turbulent fluid, and its time-frequency representation. Right: acceleration, velocity and trajectory, reconstructed for two components from the measurement of velocity by Doppler effect.

random cascades because they measure statistical quantities of stationary signals with relevant self-similar properties but no inner oscillations [ABJM98, Jaf04].

2. Time evolution and Fourier analysis: modern Lagrangian and vorticity measurements are made possible by following the instant variation of the Fourier spectrum of some nonstationary signal. Neither the temporal nor the spectral representation is enough: time-frequency representations that unfold the informations jointly in time and frequency [Fla93] are needed.

   A linear time-frequency decomposition is achieved in the same manner as the wavelet transform, using a basis built by shifts in time and frequency of a small wave packet: $v(t) = \iint r_v(u,\nu) b_{uf}(t) \mathrm{d}u\mathrm{d}f$, with $b_{uf}(t) = b_0(t-u)e^{-i2\pi f t}$. The variable ν is indeed a frequency and $r_v(u,\nu)$ gives the component of v at frequency ν and time u. The time-frequency spectrum is $\mathbb{E}\left\{|r_v(u,\nu)|^2\right\}$ Note that instead of time and frequency shifts, the wavelet transform uses time-shifts and dilation on the mother wavelet, so that the variables are time and scale rather than of time and frequency. If one is interested in the time-frequency spectrum, it is possible to achieve better estimation using bilinear densities that are time-frequency decompositions of the energy, instead of the signal. They are derived from the Wigner-Ville distribution: $W_v(t,f) = \int v(t+\tau/2)v^*(t-\tau/2)e^{-i2\pi f\tau}\mathrm{d}\tau$, applying some smoothing in time and/or frequency. Representations of this kind are used to analyse hereafter the non-stationary signals of Lagrangian experiments and of vorticity measurements.

3. Self-similarity and inner geometry: we would like to describe at the same time oscillations and self-similar exponents. It is known that wavelets are not well adapted to study oscillations [ABJM98]. A variant is measuring geometry in a nonstationary context (self-similarity implies non-stationarity). Ad-hoc procedures constructed on the wavelet transform [KV94] or on the Mellin-time representations [Bor02] were considered, but for now with no positive result. The second part of this chapter is devoted to the Mellin representation that is adapted to probe self-similarity and some features of geometry because it is based on self-similar oscillating functions $(t-t_0)^{h+i\alpha}$. We will sketch the possibilities offered by this representation, alternative to the Fourier representation.

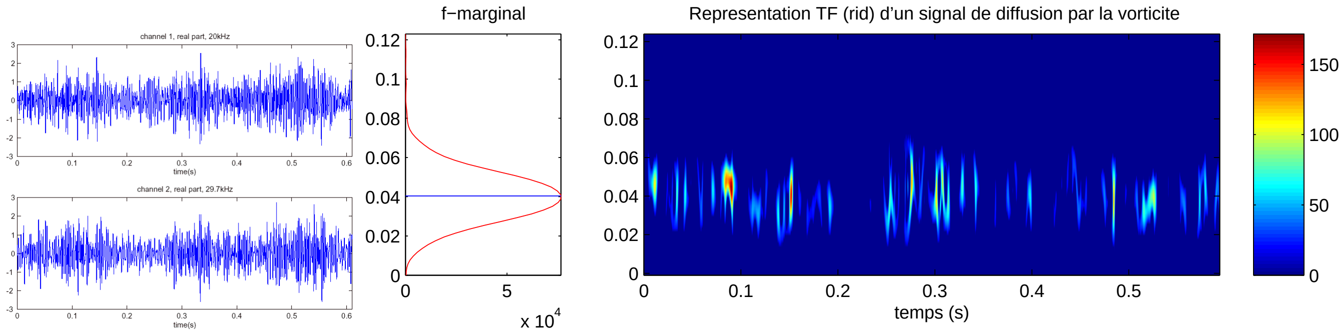

Figure 4: Measurement of vorticity by acoustic scattering [BMW99]. Left: examples of recorded signals for two different scattered waves at the same time by the same volume: they both represent the same $\tilde{\boldsymbol{\omega}}_i(\mathbf{k}, t)$ along time t. Right: quadratic time-frequency representation of one signal, exhibiting packets of structured vorticity advected through the measurement volume. [BMW99]

Measurements of Lagrangian velocity. Recent experiments have been able to track solid particles released in a turbulent fluid and record their Lagrangian velocities $\mathbf{u}(t)$ [LVC$^+$01, MMMP01]. First experiment uses high-speed detectors to record the trajectories, and the second one tracks them by sonar methods. In both cases the measurement deals with a non-stationary signal that should be tracked in position and value along time. In the experiment [MMMP01], ultra-sonor waves are reflected by the particle and the Doppler effect catches its velocity. The figure 3 shows a sample experimental signal whose instantaneous frequency is the instant Lagrangian velocity. A time-frequency analysis allow to follow the frequency and thus $u(t)$. Acceleration, velocity and trajectory is reconstructed from this data (for two components).

The signals contain many oscillating events such as the one figured here, and many more trajectories which are almost smooth and ballistic between short periods with strong accelerations. This is consistent with the existence of a few swirling structure but a clear connexion between oscillations and intermittency is not made. By now, statistical analysis of the datas show that Lagrangian velocity is intermittent [MMMP01], with an intermittency described well by a multifractal model analog to the one used for Eulerian velocity [CRL$^+$03].

Measurements of vortices and of vorticity. Intead of trying to find indirect effects of the vortices, it was tried to study directly the intermittency of turbulence in the vorticity domain. Measuring locally vorticity is difficult and by now not reliable. Using the sound scattering property of vorticity, and acoustic spectroscopy method was developped [BMW99].

The method measures a time-resolved Fourier component of vorticity, $\tilde{\boldsymbol{\omega}}_i(\mathbf{k}, t) = \int \boldsymbol{\omega}_i(\mathbf{r}, t) e^{-i2\pi\mathbf{k}\cdot\mathbf{r}} \mathrm{d}\mathbf{r}$, summed all over some spatial volume. Figure 4 shows recorded signals of scattering amplides for two different incident waves; they look alike because both are measure of the same quantity, $\tilde{\boldsymbol{\omega}}_i(\mathbf{k}, t)$. The intermittency of the signal is the existence of bursts of vorticities that cross the measurement volume; those packets are also characteristic of some structuration of vorticity, mayhap as vortices. They are evidenced on the time-frequency decomposition of one signal on the right. The intermittency is well captured by the description of a slow non-stationary activity that drives many short-time bursts, and so causes multi-scale properties [PMG$^+$04].

To conclude this introduction to turbulence, let us summarize the complexity of fluid turbulence. The problem is driven by a non-linear PDE that is reluctant to mathematical analysis, so that theories are mainly phenomelogy and stochastic modelling of the velocity (or vorticity). The signals are irregular, intermittent and one would like to question their self-similar aspects, their non-stationary properties, and their geometrical organization. Because there exists no single method that capture all these features, mutiple tools of signal processing are useful.

2 Mellin representation for stochastic processes

In this second part, we detail a signal processing method that use oscillating functions as basis functions: the Mellin transformation. Its interest is that it is encompasses both self-similar and oscillating properties in one description. We will survey some properties that are useful for signal representation and processing.

2.1 Dilation and Mellin representation

We aim at finding a formalism suited to scale invariance. Let us recall the definition of self-similarity: it is a statistical invariance under the action of dilations. Let $\mathcal{D}_{H,\lambda}$ be a dilation of scale ratio λ so that $(\mathcal{D}_{H,\lambda}X)(t) = \lambda^{-H}X(\lambda t)$. The exponent H specifies one group of dilation, $\{\mathcal{D}_{H,\lambda}, \lambda \in \mathbb{R}_*^+\}$ which is a continuous unitary representation of $(\mathbb{R}_*^+, \times)$ in the space $L^2(\mathbb{R}_*^+, t^{-2H-1}\mathrm{d}t)$. The harmonic analysis associated to this group is the Mellin reprenstation. Indeed, the hermitian generator of this group is $\mathcal{C}$ defined as: $i2\pi(\mathcal{C}X)(t) = (-H + t\mathrm{d}/\mathrm{d}t)X(t)$, so that $\mathcal{D}_{H,\lambda} = e^{i2\pi\lambda\mathcal{C}}$. The operator $\mathcal{C}$ characterizes a scale because its eigenfunctions are unaffected by scale changes (dilations), so the eigenvalues are a possible measure of scale. Those eigenvalues $E_{H,\beta}(t)$ satisfy $\mathrm{d}E_{H,\beta}(t)/E_{H,\beta}(t) = (H + i2\pi\beta)\mathrm{d}t/t$, thus $E_{H,\beta}(t) = t^{H+i2\pi\beta}$ up to a multiplicative constant. One obtains the basis of Mellin functions with associated representation:

$$(\mathcal{M}_H X)(\beta) = \int_0^{+\infty} t^{-H-i2\pi\beta} X(t)\frac{\mathrm{d}t}{t} \text{ and } X(t) = \int_{-\infty}^{+\infty} E_{H,\beta}(t)(\mathcal{M}_H X)(\beta)\mathrm{d}\beta. \tag{5}$$

A signal processing view of several applications the Mellin transform may be found in [Coh93, BBO96, Fla98, Nic02], and mathematical aspects are documented in [Dav84, Zem87]. Relevant features here are first that β is a meaningful scale, second the oscillating aspects of the Mellin functions $E_{H,\beta}(t)$. Those functions are chirps of instantaneous frequency β/t. See a drawing of such a function on figure 5. One can disregard the behaviour of those functions near 0; the important feature is the chirp part and it holds even if the function is filtered by some window, as seen on this figure. By this means we may describe both self-similarity and some oscillations, as long as they can be well approximated by smoothed Mellin function, of the form $g(t)|t - t_0|^{H+i2\pi\beta}$.

2.2 Interpretation for self-similarity

A random process $\{X(t), t \in \mathbb{R}_*^+\}$ is self-similar with exponent H (H-ss) and only if for any $\lambda \in \mathbb{R}_*^+$, one has $\{(\mathcal{D}_{H,\lambda}X)(t), t \in \mathbb{R}_*^+\} \stackrel{d}{=} \{X(t), t \in \mathbb{R}_*^+\}$ [Ver87]. Giving the definition of self-similarity [Lam62], J. Lamperti noticed a specific property of the invertible transformation $\mathcal{L}_H$, now called Lamperti transformation and defined as:

$$(\mathcal{L}_H Y)(t) = t^H Y(\log t),\ t > 0 \qquad \text{and} \qquad (\mathcal{L}_H{}^{-1}X)(t) = e^{-Ht}X(e^t),\ t \in \mathbb{R} \tag{6}$$

This transformation maps stationary processes onto self-similar processes, and the converse for its inverse. Stationarity is the invariance under time-shifts; if Y is stationary, one has: $(\mathcal{S}_\tau Y)(t) \hat{=} Y(t+\tau) \stackrel{d}{=} Y(t)$ for any $\tau \in \mathbb{R}$. The Lamperti transformation is a unitary equivalence between the group of $\mathcal{S}_\tau$ and the group of dilations $\mathcal{D}_{H,\lambda}$:

$$\mathcal{L}_H{}^{-1}\mathcal{D}_{H,\lambda}\mathcal{L}_H = \mathcal{S}_{\log\lambda} \qquad \text{and} \qquad \mathcal{L}_H\mathcal{S}_\tau\mathcal{L}_H{}^{-1} = \mathcal{D}_{H,e^\tau}. \tag{7}$$

This equivalence has interesting consequences: a natural representation of a self-similar process X is to use its stationary generator $\mathcal{L}_H{}^{-1}X$. Signal processing for stationary signals is a well-known field and methods can then be converted in tools for self-similar processes by applying equivalence (7) [FBA03, BFA02]. In this contexte, Mellin representation is suited to H-ss processes in the same way as Fourier representation is suited to stationary processes, because $\mathcal{M}_H = \mathcal{F}\mathcal{L}_H{}^{-1}$:

$$(\mathcal{F}\mathcal{L}_H{}^{-1}X)(\beta) = \int_{-\infty}^{+\infty} (\mathcal{L}_H{}^{-1}X)(u)e^{-i2\pi\beta u}\mathrm{d}u = \int_0^{\infty} t^{-H}X(t)t^{-i2\pi\beta-1}\mathrm{d}t = (\mathcal{M}_H X)(\beta) \tag{8}$$

For instance, time-frequency methods that were suited to measure jointly time and frequency components of a signal will be converted in time-Mellin scale representations that measure contents as a joint function of time and Mellin scale.

2.3 Spectral analysis of self-similar processes

• **Covariance and spectrum.** A H-ss process $X(t)$ has a covariance that reads necessarily as: $R_X(t,s) \hat{=} \mathbb{E}\{X(t)X(s)\} = (ts)^H c_X(t/s)$. This comes from the correlation function $\gamma_Y(\tau)$ of its stationary generator $Y = (\mathcal{L}_H{}^{-1}X)$, with $\gamma_Y(\log k) = c_X(k)$. The Mellin spectral density $\Xi_X(\beta)$ of X is then simply introduced by means of the spectrum of Y:

$$\Gamma_Y(\beta) = \int_{-\infty}^{+\infty} \gamma_Y(\tau) e^{-i2\pi\beta\tau} \mathrm{d}\tau = \int_0^{+\infty} c_X(k) k^{-i2\pi\beta-1} \mathrm{d}k = (\mathcal{M}_0 c_X)(\beta) \hat{=} \Xi_X(\beta). \tag{9}$$

H-ss processes admit also an harmonizable decomposition on the Mellin basis so that $X(t) = \int t^{H+i2\pi\beta} \mathrm{d}\underline{X}(\beta)$, with decorrelated spectral increments. Thus we have $\mathbb{E}\{\mathrm{d}\underline{X}(\beta_1)\overline{\mathrm{d}\underline{X}(\beta_2)}\} = \delta(\beta_1-\beta_2)\,\Xi_X(\beta_1)\mathrm{d}\beta_1\mathrm{d}\beta_2$.
• **Scale invariant linear systems.** A linear operator $\mathcal{G}$ is covariant for dilations if it satisfies $\mathcal{G}\mathcal{D}_{H,\lambda} = \mathcal{D}_{H,\lambda}\mathcal{G}$ for any scale ratio $\lambda \in \mathbb{R}_*^+$. Using equation (7), we may remplace $\mathcal{D}_{H,\lambda}$ by $\mathcal{S}_{\log\lambda}$ and we obtain the equality: $(\mathcal{L}_H{}^{-1}\mathcal{G}\mathcal{L}_H)\mathcal{S}_{\log\lambda} = \mathcal{S}_{\log\lambda}(\mathcal{L}_H{}^{-1}\mathcal{G}\mathcal{L}_H)$. Thus, $\mathcal{L}_H{}^{-1}\mathcal{G}\mathcal{L}_H = \mathcal{H}$ is a linear stationary operator, so it acts as a filter by means a convolution. The Lamperti transformation maps addition to multiplication so that $\mathcal{G}$ will act by means of a multiplicative convolution instead of the usual one:

$$(\mathcal{G}X)(t) = \int_0^{\infty} g(t/s)X(s)\frac{\mathrm{d}s}{s} = \int_0^{\infty} g(s)X(t/s)\frac{\mathrm{d}s}{s}. \tag{10}$$

Let us consider $A = \mathcal{G}X$ with $\{X(t), t > 0\}$ and H-ss process and $\mathcal{G}$ a scale invariant filter. Then $A(t)$ is also self-similar because $\mathcal{D}_{H,\lambda}A = \mathcal{D}_{H,\lambda}\mathcal{G}X = (\mathcal{G}\mathcal{D}_{H,\lambda})X = \mathcal{D}_{H,\lambda}X$. If the covariance of X is given by c_X, then a formula of interferences gives the covariance of A: $c_A(k) = \int c_X(u)\rho_g(k/u)\mathrm{d}u/u$, introducing here the Mellin correlation of the function g: $\rho_g(\lambda) = \int g(\lambda s)\overline{g(s)}s^{-2H-1}\mathrm{d}s$. The corresponding property for the Mellin spectrum is a multiplication: $\Xi_A(\beta) = |(\mathcal{M}_H g)(\beta)|^2\,\Xi_X(\beta)$.
• **Representation by scale invariant filters.** By means of the Bochner theorem, any H-ss process is the output of a scale-invariant linear system:

$$X(t) = \int_0^{+\infty} g(t/s)V(s)\frac{\mathrm{d}s}{s}, \text{ with } \mathbb{E}\left\{V(t)\overline{V(s)}\right\} = \sigma^2 t^{2H+1}\delta(t-s). \tag{11}$$

The random noise $V(t)$ is white and Gaussian but nonstationary; it is the image by $\mathcal{L}_H$ of the Wiener process. The self-similar process X is defined by g; the second-order properties are covariances given by means of $c_X(k) = \sigma^2 k^{-H}\int g(k\theta)\overline{g(\theta)}\theta^{-2H-1}\mathrm{d}\theta$, and Mellin spectrum which is $\Xi_X(\beta) = \sigma^2|(\mathcal{M}_H g)(\beta)|^2$. A further step is to study parametric models of self-similar processes by taking $(\mathcal{M}_H g)(\beta)$ as a rational fraction. One can show that $X(t)$ is in this case the solution of a Euler-Cauchy system: $\sum_{n=0}^p \alpha_n t^n X^{(n)}(t) = \sum_{n=0}^q \beta_n t^n V^{(n)}(t)$. Models of this kind were studied in [YK97, NG99].

2.4 Examples of Mellin representation

Fractional Brownian motions. A fractional Brownian motions is defined as a Gaussian, H-ss process with stationary increments [MV68]. Its covariance is necessarily: $R_{B_H} = \sigma^2(|t|^{2H} + |s|^{2H} - |t-s|^{2H})/2$ which satisfies the general expected structure with $c_{B_H}(k) = \sigma^2[k^H + k^{-H} - |\sqrt{k} - 1/\sqrt{k}|^{2H}]/2$. The corresponding Mellin spectrum is obtained by a straightforward calculus ($\mathbf{\Gamma}$ is the Euler function):

$$\Xi_{B_H}(\beta) = \frac{\sigma^2}{H^2 + 4\pi^2\beta^2}\left|\frac{\mathbf{\Gamma}(1/2 + i2\pi\beta)}{\mathbf{\Gamma}(H + i2\pi\beta)}\right|^2. \tag{12}$$

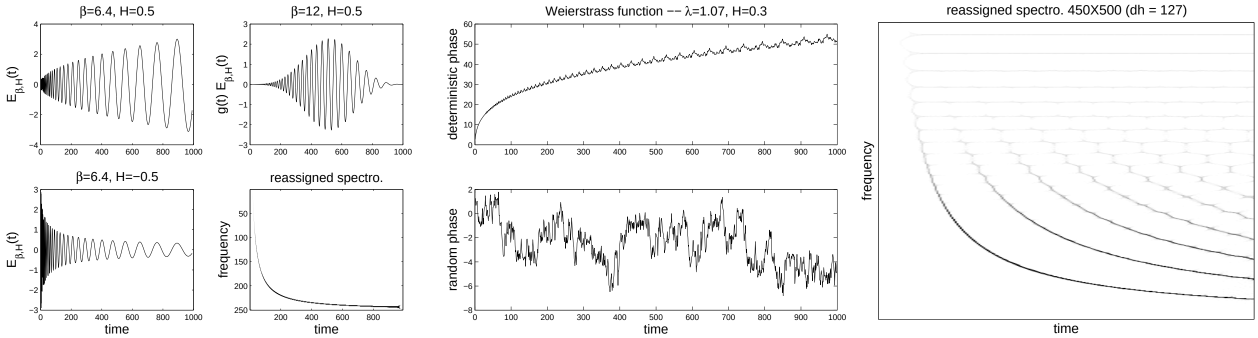

Figure 5: Left: some Mellin functions with various H, with a reassigned spectrogram of an smoothed Mellin function (where $g(t)$ is a Kaiser window) that shows the chirp behaviour of the Mellin functions. Middle: samples of Weierstrass-Mandelbrot functions, both deterministic and random ($H = 0.3$, $\lambda = 1.07$). Right: reassigned spectrogram of the empirical variogram of a Weierstrass-Mandelbrot function (adapted fom [FB03]). See the text for interpretation.

Here, we have a representation of fractional Brownian motions alternative to its harmonic or moving-average representations. The Barnes-Allan [BA66] model, known to be close to B_H, has exactly the same Mellin spectrum that B_H. From this spectral representation, one can synthetize exact samples of fractional Brownian motions: it is enough to prescribe Mellin spectral increments satisfying equation (12) with random i.i.d. phases in $[0, 2\pi[$. An inverse Mellin transform gives then a fractional Brownian motion. Classical methods of whitening, prediction and interpolation for this process were derived from this Mellin representation in [NP99, NP00]. Developments of the synthesis method from the Mellin spectrum for other self-simiilar processes without stationary increments were studied also in [Bor02].

The Weiertrass-Mandelbrot function. This function is a good model of inexact self-similarity that can be studied by means of a Mellin decomposition. It is defined [BL80] as $W(t) = \sum_{n\in\mathbb{Z}} \lambda^{-nH}(1 - e^{i\lambda^n t})e^{i\phi_n}$, with i.i.d. phases ϕ_n. The function is given here as a sum of Fourier modes this is possible because it has stationary increments. But another feature is more obvious if one considers its decompostion on a Mellin basis: its scale invariance. $W(t)$ has Discrete Scale Invariance [BFA02] because $W(\lambda^k t) \overset{d}{=} \lambda^{-kH} W(t)$, scale invariance for dilations with a scale ratio that is a power of λ only. Using $\mathcal{L}_H$, one can find up the Mellin representation for the deterministic version of the function, with $\phi_n = 0$, [BL80, FB03]: $W(t) = \sum_m \frac{-\boldsymbol{\Gamma}(-H-m/\ln\lambda)}{\ln\lambda} e^{[-i\pi(H+m/\ln\lambda)/2]} E_{H,m/\ln\lambda}(t)$.

The two writings of $W(t)$ give first its time-frequency representation then its time-Mellin scale representation. In this case, both methods of analysis are valid as tools to measure the characteristics of the function. The relevance comes from the joint properties of stationary increments and self-similarity (even in the weakened sense of Discrete Scale Invariance). A time-frequency analysis illustrates this, see figure 5. Deterministic and randomized versions of $W(t)$ have a spectrogram (from the detrended empirical variogram) that is made partly of pure tones, and partly of chirps, that are localized on the Mellin modes $\beta = m/\ln\lambda$. Here both aspects are showh, depending on the width of the smoothing window with respect to the rapidity of variation of the chirp (one see the chirp when its frequency does not change quickly over the length of the window) [FB03].

Concluding remarks. We lectured here a signal processing view of turbulence. We have surveyed how the complexity of turbulence, and the need to understand various models and experiments, is linked to a great diversity of signal processing methods that are useful for turbulence: time-scale analysis, time-frequency analysis, self-similarity and geometry analysis.

Concerning the last point, we are far from having at disposal convenient tools for estimation of the geometry (fractal sets, oscillations,...) of a self-similar process. We have proposed here a framework adapted to self-similarity and based on the oscillating Mellin functions $t^{h+i2\pi\beta}$ but we have not yet found a tractable extension to oscillating singularities of the form $|t - t_0|^{h+i2\pi\beta}$ that could be of relevance in turbulence. The origin of time t_0 has to be a variable in the second case, whereas the Lamperti framework is for a fixed time origin of the Mellin functions. Because of that, a mixture of oscillating functions such as $|t - t_0|^{h+i2\pi\beta}$ may have multifractal properties close to the one measured in turbulence but one lack signal processing tools to inverse the mixture and estimates the various parameters (t_0, h, β) of each object.

Finally, turbulence is still an active and open field with many problems that are interesting from a mathematical, physical or signal processsing point of view. This is a subject where one needs to establish fruitful interactions between models, tools of analysis and measurements.

Thanks. I would like to thank people that made this work possible by their competence and their willingness to share their knowledge and their ideas. I thank espcially Olivier Michel, Patrick Flandrin and Pierre-Olivier Amblard, with whom I have the pleasure to work. I am also thankful to C. Baudet, B. Castaing, N. Mordant, J.F. Pinton, and J.C. Vassilicos, all of them who taught me the few things I know about turbulence.

References

[ABJM98] A. Arneodo, E. Bacry, S. Jaffard, and J.F. Muzy. Singularity spectrum of multifractal functions involving oscillating singularities. *J. Four. Anal. Appl.*, 4(2):159–174, 1998.

[AFTV00] P. Abry, P. Flandrin, M. Taqqu, and D. Veitch. Wavelets for the analysis, estimation, and synthesis of scaling data. In K. Park and W. Willinger, editors, *Self-Similar Network Traffic and Performance Evaluation*. Wiley, 2000.

[AM95] A. Arneodo and E. Bacry J.F. Muzy. The thermodynamics of fractals revisited with wavelets. *Physica A*, 213:232–275, 1995.

[BA66] J. Barnes and A. Allan. A statistical model of flicker noise. *Proc. IEEE*, 54:176–178, 1966.

[Bat53] G.K. Batchelor. *The theory of homogeneous turbulence*. Cambridge University Press, 1953.

[Bat67] G.K. Batchelor. *An introduction to fluid dynamics*. Cambridge University Press, 1967.

[BBO96] J. Bertrand, P. Bertrand, and J.P. Ovarlez. The Mellin transform. In A.D. Poularikas, editor, *The Transforms and Applications Handbook*. CRC Press, 1996.

[BCT+93] R. Benzi, S. Ciliberto, R. Tripicione, C. Baudet, and F. Massaioli. Extended self-similarity in turbulent flows. *Phys. Rev. E*, 48:R29–R32, 1993.

[BFA02] P. Borgnat, P. Flandrin, and P.-O. Amblard. Stochastic discrete scale invariance. *Signal Processing Lett.*, 9(6):181–184, June 2002.

[BL80] M. Berry and Z. Lewis. On the Weierstrass-Mandelbrot fractal function. *Proc. Roy. Soc. Lond. A*, 370:459–484, 1980.

[BLF53] A. Blanc-Lapierre and R. Fortet. *Théorie des fonctions aléatoires*. Masson, Paris, 1953.

[BM03] E. Bacry and J.F. Muzy. Log-infinitely divisible multifractal processes. *Comm. in Math. Phys.*, 236:449–475, 2003.

[BMW99] C. Baudet, O. Michel, and W. Williams. Detection of coherent vorticity structures using time-scale resolved acoustic spectroscopy. *Physica D*, 128:1–17, 1999.

[Bor02] Pierre Borgnat. *Modèles et outils pour les invariances d'échelle brisée : variations sur la transformation de Lamperti et contributions aux modèles statistiques de vortexen turbulence*. PhD thesis, École normale supérieure de Lyon, November 2002.

[Cas97] B. Castaing. Turbulence: Statistical approach. In B. Dubrulle, F. Graner, and D. Sornette, editors, *Scale Invariance and Beyond*, pages 225–234. Springer, 1997.

[CBC95] G. Chavarria, C. Baudet, and S. Ciliberto. Hierarchy of the energy dissipation moments in fully developed turbulence. *Phys. Rev. Lett.*, 74:1986–1989, 1995.

[Che04] L. Chevillard. *Description multifractale unifiée du phénomène d'intermittenceen turbulence eulérienne et lagrangienne*. PhD thesis, Université Bordeaux I, 2004.

[Coh93] L. Cohen. The scale representation. *IEEE Trans. on Signal Proc.*, 41(12):3275–3292, December 1993.

[CRA04] P. Chainais, R. Riedi, and P. Abry. On non scale invariant infinitely divisible cascades. to appear in IEEE Trans. on Info. Theory, 2004.

[CRL$^+$03] L. Chevillard, S. Roux, E. Lévêque, N. Mordant, J.F. Pinton, and A. Arneodo. Lagrangian velocity statistics in turbulent flows: Effects of dissipation. *Phys. Rev. Lett.*, 91:214502, 2003.

[Dav84] B. Davies. *Integral transforms and their applications*. Springer-Verlag, New York, 1984.

[DCB91] S. Douady, Y. Couder, and M.E. Brachet. Direct observation of the intermittency of intense vorticity filaments in turbulence. *Phys. Rev. Lett.*, 67:983–986, 1991.

[FB03] P. Flandrin and P. Borgnat. On the chirp decomposition of Weierstrass-Mandelbrot functions, and their time-frequency interpretation. *Applied and Computational Harmonic Analysis*, 15:134–146, September 2003.

[FBA03] P. Flandrin, P. Borgnat, and P.-O. Amblard. From stationarity to self-similarity, and back : Variations on the Lamperti transformation. In G. Raganjaran and M. Ding, editors, *Processes with Long-Range Correlations: Theory and Applications*, volume 621 of *Lectures Notes in Physics*, pages 88–117. Springer-Verlag, June 2003.

[Fla93] P. Flandrin. *Temps-Fréquence (1ère ed.)*. Hermes, 1993.

[Fla98] P. Flandrin. Inequalities in Mellin-Fourier signal analysis. Newton Institute Preprint NI98030-NSP, Cambridge, UK, November 1998.

[FM81] U. Frisch and R. Morf. Intermittency in nonlinear dynamics and singularities at complex times. *Phys. Rev. A*, 23(5):2673–2705, May 1981.

[FMW03] U. Frisch and M. Mineev-Weinstein. Extension of the pole decomposition for the multidimensional Burgers equation. *Phys. Rev. E*, 67:067301, 2003.

[FP85] U. Frisch and G. Parisi. On the singularity structure of fully developped turbulence. In M. Ghil, R. Benzi, and G. Parisi, editors, *Proc. of Int. School of Phys. on Turbulence and predictability in geophysical fluid dynamics*, pages 84–87, Amsterdam, 1985. North-Holland.

[Fri95] U. Frisch. *Turbulence*. CUP, Cambridge, 1995.

[Gag87] Y. Gagne. *Étude expérimentale de l'intermittence et des singularités dans le plan complexe en turbulence développée*. PhD thesis, INP Grenoble, 1987.

[Jaf97] S. Jaffard. Multifractal formalism for functions, part 1 and 2. *SIAM J. of Math. Anal.*, 28(4):944–998, 1997.

[Jaf04] S. Jaffard. Wavelet techniques in multifractal analysis. Proceedings of Symposia in Pure Mathematica, 2004.

[JKVF93] J.C.R. Hunt, N.K.-R. Kevlahan, J.C. Vassilicos, and M. Farge. Wavelets, fractals and fourier transforms: detection and analysis of structures. In M. Farge, J.C.R. Hunt, and J.C. Vassilicos, editors, *Wavelets, Fractals, and Fourier Transforms*, pages 1–38. Oxford : Clarendon Press, 1993.

[Kol41a] A.N. Kolomogorov. The local structure of turbulence in incompressible viscuous fluid for very large Reynolds numbers. *Dokl. Akad. Nauk SSSR*, 30:9–13, 1941.

[Kol41b] A.N. Kolomogorov. On degeneration of isotropic turbulence in a incompressible viscuous liquid. *Dokl. Akad. Nauk SSSR*, 31:538–540, 1941.

[KP75] J.P. Kahane and J. Peyrière. Sur certaines martingales de Benoit Mandelbrot. *Adv. Math.*, 22:131–145, 1975.

[KV94] N. Kevlahan and J.C. Vassilicos. The space and scale dependencies of the self-similar structure of turbulence. *Proc. R. Soc. Lond. A*, 447:341–363, 1994.

[Lam62] J. Lamperti. Semi-stable stochastic processes. *Trans. Amer. Math. Soc.*, 104:62–78, 1962.

[Las04] B. Lashermes. PhD thesis, ÉNS Lyon, in preparation, 2004.

[Lun82] T.S. Lundgren. Strained spiral vortex model for turbulent fine structure. *Phys. Fluids*, 25(12):2193–2203, 1982.

[LVC$^+$01] A. La Porta, G.A. Voth, A.M. Crawford, J. Alexander, and E. Bodenschatz. Fluid particle accelerations in fully developped turbulence. *Nature*, 409:1017–1019, 2001.

[Mey90] Y. Meyer. *Ondelettes et opérateurs*. Hermann, 1990.

[MMMP01] N. Mordant, P. Metz, O. Michel, and J.F. Pinton. Scaling and intermittency of Lagrangian velocity in fully developped turbulence. *Phys. Rev. Lett.*, 87:21–24, 2001.

[Mof84] H. Moffatt. Simple topological aspects of turbulent velocity dynamics. In T. Tatsumi, editor, *Turbulence and chaotic phenomena in fluids*, pages 223–230. Elsevier, 1984.

[Mof93] H. Moffatt. Spiral structures in turbulent flows. In M. Farge, J.C.R. Hunt, and J.C. Vassilicos, editors, *Wavelets, Fractals, and Fourier Transforms*, pages 317–324. Oxford : Clarendon Press, 1993.

[MV68] B. Mandelbrot and J. W. Van Ness. Fractional Brownian motions, fractional Brownian noises and applications. *SIAM review*, 10:422–437, 1968.

[MY71] A.S. Monin and A.S. Yaglom. *Statistical fluid mechanics (vol. 1 and 2)*. The MIT Press, 1971.

[NG99] E. Noret and M. Guglielmi. Modélisation et synthèse d'une classe de signaux auto-similaires et à mémoire longue. In *Proc. Conf. Delft (NL) : Fractals in Engineering*, pages 301–315. INRIA, 1999.

[Nic02] J.M. Nicolas. Introduction aux statistiques de deuxième espèce : Applications aux lois d'images SAR. Rapport interne, ENST, Paris, February 2002.

[Nov71] E.A. Novikov. Intermittency and scale-similarity in the structure of a turbulent flow. *P.M.M. Appl. Math. Mech.*, 45:231–241, 1971.

[NP99] C. Nuzman and V. Poor. Transformed spectral analysis of self-similar processes. In *Proc. CISS'99*, May 1999.

[NP00] C. Nuzman and V. Poor. Linear estimation of self-similar processes via Lamperti's transformation. *J. of Applied Probability*, 37(2):429–452, June 2000.

[PMG$^+$04] C. Poulain, N. Mazelllier, P. Gervais, Y. Gagne, and C. Baudet. Lagrangian vorticity and velocity measurements in turbulent jets. *Flow, Turbulence, and Combustion*, 72(2–4):245–271, 2004.

[PPB$^+$03] S. Pietropinto, C. Poulain, C. Baudet, B. Castaing, B. Chabaud, Y. Gagne, B. Hébral andY. Ladam, P. Lebrun, O. Pirotte, and P. Roche. Superconducting instrumentation for high Reynolds turbulence experiments with low temperature gaseous helium. *Physica C*, 386:512–516, 2003.

[SP96] P.G. Saffman and D.I. Pullin. Calculation of velocity structure fonctions for vortex models of isotropic turbulence. *Phys. Fluids*, 8(11):3072–3077, 1996.

[Ver87] W. Vervaat. Properties of general self-similar processes. *Bull. of International Statistical Inst.*, 52:199–216, 1987.

[YK97] B. Yazici and R. L. Kashyap. A class of second-order stationary self-similar processes for $1/f$ phenomena. *IEEE Trans. on Signal Proc.*, 45(2):396–410, 1997.

[Zem87] A. Zemanian. *Generalized integral transforms*. Dover, 1987.